

A Microfluidic Device for Kinetic Optimization of Protein Crystallization and *In Situ* Structure Determination

Carl L. Hansen,[†] Scott Classen,[†] James M. Berger,[†] and Stephen R. Quake^{*†}

Department of Applied Physics, California Institute of Technology, 1200 East California Boulevard, Pasadena, California 91125

Received November 10, 2005; E-mail: quake@stanford.edu

Recently microfluidic technologies have emerged as viable platforms for nano-volume protein crystallization screening.^{1–4} In particular, screening in nanoliter volume free interface diffusion (FID) reactors has been instrumental in the crystallization of a broad range of targets that had proven to be intractable by conventional screening techniques and has been successfully incorporated into academic and industrial structural biology efforts.^{5,6} However, crystals grown in nanoliter volume reactors may be of insufficient size for diffraction studies, and scale-up usually depends on growth kinetics that vary with reactor details.^{3,5} Moreover, previously reported microfluidic crystallization devices do not allow the post-crystallization addition of cryoprotectant necessary for diffraction studies at cryogenic temperatures.¹¹

In this paper, we report a microfluidic device which provides a link between chip-based nanoliter volume crystallization screening and structure analysis through “kinetic optimization” of crystallization reactions and *in situ* structure determination. Kinetic optimization of mixing rates through systematic variation of reactor geometry and actuation of micromechanical valves is used to screen a large ensemble of kinetic trajectories that are not practical with conventional techniques. Using this device, we demonstrate control over crystal quality, reliable scale-up from nanoliter volume reactions, facile harvesting and cryoprotectant screening, and protein structure determination at atomic resolution from data collected in-chip.

The basic structure of the kinetic optimization device implements five parallel, FID reaction chambers⁷ encased beneath a semipermeable membrane at the bottom of a macroscopic fluid reservoir. The FID reactors equilibrate not only with themselves via diffusion but also with reservoir solutions through the membrane, which defines an osmotic bath that controls both the rate and extent of vapor transport to and from the reactors. The combined FID–vapor diffusion motif (Figure 1) is repeated 20 times on the chip; each version has different channel lengths and volumes. The device has channel lengths ranging from 300 to 2400 μm , thereby allowing the characteristic mixing time to be varied by a factor of 8.⁷

The present device further allows control over the rate and extent of water vapor transport through the permeable poly(dimethylsiloxane) (PDMS) membrane.⁸ The extent of dehydration can be directly regulated by filling the wells overlying each reaction site with a solution of well-defined vapor pressure and sealed with clear adhesive tape. Over the course of FID-driven crystallization, water in the well solution passes through the membrane by vapor diffusion, equilibrating with the contents of the reactor until the

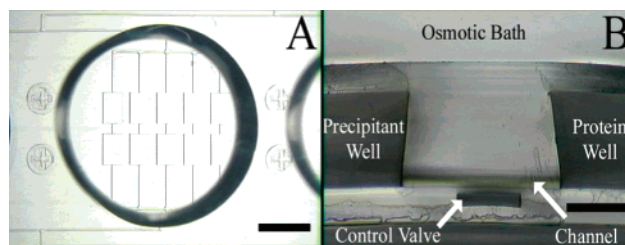


Figure 1. Optical micrographs of microreactors for combined FID and vapor diffusion crystallization. (A) Reaction site enclosed within a 250 μm thick PDMS membrane located at the bottom of a 150 μL reservoir well. Scale bar is 2000 μm . (B) Cross-section of a μFID reactor fabricated in a 250 μm thick semipermeable elastomer membrane. Scale bar is 150 μm .

osmotic potentials of both solutions match. In a second approach, the dehydration rates of the FID reactors were controlled by dispensing semipermeable fluorinated oil (poly-3,3,3-trifluoropropylmethylsiloxane; Hampton Research) into each reservoir, thereby creating a variable impedance to vapor transport. Rates of vapor transport were then systematically varied by changing oil levels in the wells.

We applied kinetic optimization of mixing rates to the crystallization growth of four model proteins—lysozyme, ferritin, insulin, and catalase—using fixed chemical parameters. Reactors with the shortest channel length (and hence fastest mixing rates) exhibited more rapid crystal formation, an increased number of nucleation events, and smaller mean crystal size. The dependence of the number of nucleation events on channel length for fixed mixing ratio and osmotic bath strength is shown for lysozyme, ferritin, and insulin (Figure 2A). Strikingly, in addition to controlling the number of crystal nucleation events and maximum crystal size, modulation of equilibration kinetics affected crystal habit as well (Figure 2C). These studies demonstrate the dependence of crystal nucleation, growth, and morphology on kinetic trajectory^{9,10} and also highlight the ability of controlled kinetic optimization to regulate protein crystallization.

Microchannel valves can further be closed and reopened at will, thus halting or restarting FID at user-defined points in time. Operating FID reactors at varying duty cycles by periodically cycling valves on and off allows the rate of diffusive equilibration to be tuned continuously and systematically during an experiment. Similarly, the osmotic bath solutions can be changed arbitrarily without disturbing crystallization reactions. Together, these abilities may be used to investigate a broad set of kinetic trajectories for crystal nucleation and growth that are not readily achievable in conventional crystallization formats. For instance, in experiments with lysozyme kinetic optimization using active control over diffusive equilibration allowed for the suppression of kinetically favored crystal forms and microscopic aggregates and promoted the formation of large single crystals (Figure 2B).

[†] Current addresses: (C.L.H.) Physics & Astronomy and Electrical & Computer Engineering, The University of British Columbia, Michael Smith Laboratories, 2185 East Mall, Vancouver, BC V6T-1Z4 Canada. (S.C.) Advanced Light Source, Lawrence Berkeley National Laboratory, 1 Cyclotron Road Mail Stop 6R2100, Berkeley, CA 94720-8226, USA. (J.M.B.) Molecular and Cell Biology, 327B Hildebrand Hall #3206, University of California at Berkeley, Berkeley, CA 94720-3206, USA. (S.R.Q.) Bioengineering, Stanford University, Stanford, CA 94305, USA.

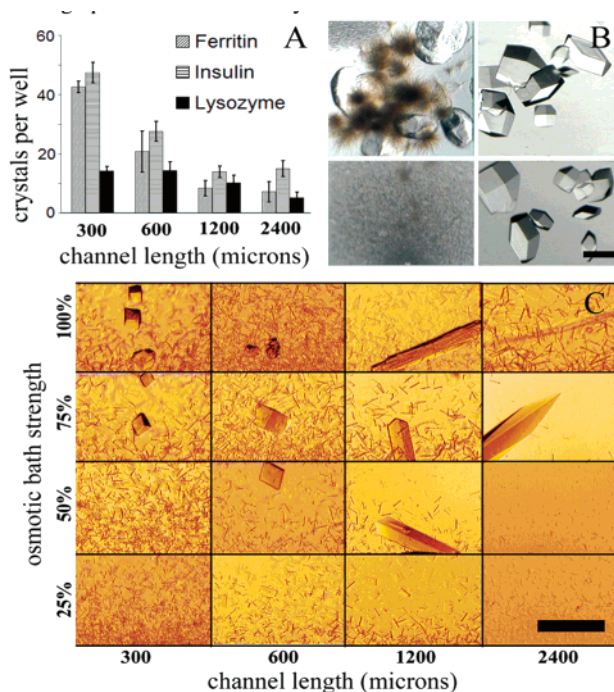


Figure 2. Screening of mixing kinetics to modulate crystal nucleation, form, and size. (A) Effect of mixing kinetics on the number of nucleation events for three model proteins. (B) Varying crystal habit under passive and active control. Optical micrographs of the crystallization of lysozyme at 4 °C using chemical and reservoir solution conditions as per panel (A). Multiple crystal forms, poorly formed crystals, and microscopic aggregation results from the passive equilibration at 2:1 and 1:1 mixing ratios (protein: precipitant) with connecting channels continuously open (left panels). Right panels of B show identical conditions incubated with valve states cycled at 11% duty cycle (15 min open followed by 2 h closed). Connecting channel lengths are 300 μm (top panels) and 600 μm (bottom panels). Scale bar is 100 μm . (C) Control of crystal size, habit, and form by regulating osmotic bath strength (between 25 and 100% of the crystallization solution) and mixing kinetics (via channel length). Three distinct morphologies are observed: thin rods, thick blades, and rhomboids. Scale bar is 150 μm .

The device was further evaluated in its ability to scale-up crystallization conditions found in 10 nL FID reactors screening chips.¹ We attempted to scale-up crystallization of a total of 14 targets, including eight well-characterized crystallization standards, three previously crystallized integral membrane proteins, one nucleic acid/protein complex, and two targets of unknown structure that only had been crystallized in 10 nL FID reactors. All 14 targets tested were successfully crystallized using chemical conditions identified in 10 nL volume reactors. This success, which occurred despite a highly varied sample pool, establishes this approach as a high correspondence method for scaling up nanoliter volume crystallization.

We used *in situ* diffraction studies to assess chip-grown crystal quality with minimal harvesting perturbations. Cryoprotectant solutions were introduced to selected reactors by diffusion over a period of 24–72 h, after which PDMS membranes containing protein crystals were punched out of the microfluidic device (Figure 3A) and mounted for X-ray analysis. *In situ* diffraction data were collected from four model proteins (lysozyme, glucose isomerase, thaumatin, and catalase) at 100 K at Beamline 12.3.1 at the Advanced Light Source (ALS).

In all cases, crystals diffracted to high resolution (<2 Å), and the data collected *in situ* from these crystals are exceeded in resolution by only a handful of the hundreds of homologous structures in the protein data bank (PDB). The general quality of

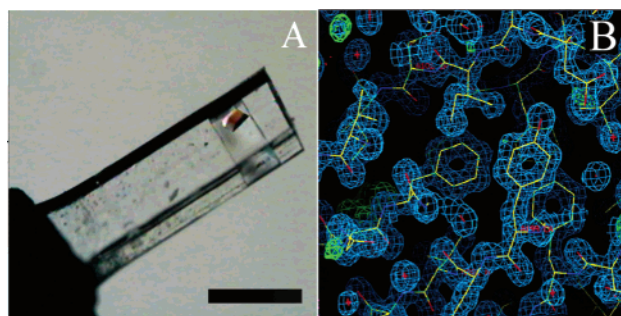


Figure 3. In-chip crystallization facilitates structure determination *in situ*. (A) Polarizing micrograph of a protein crystal mounted for *in situ* diffraction studies at room temperature. (B) $2F_o - F_c$ electron density maps (blue) contoured at 1.3σ , $F_o - F_c$ maps (green and red) contoured at $+3.5\sigma$ and -3.5σ , respectively, and refined model of thaumatin derived from 1.25 Å resolution data collected *in situ* through a PDMS membrane at Beamline 12.3.1 at the ALS (thaumatin 1, Supporting Information Table 1).

the diffraction data is also exceptional. Wilson B temperature factors are between 10 and 20 for all four datasets; R_{sym} values fall between 4.2 and 8.2%, and mosaicity values range from 0.06 to 0.2°. These studies demonstrate that kinetic optimization can yield highly ordered crystals and that high-resolution *in situ* diffraction data may be collected with minimal or no crystal damage in PDMS devices.

To further validate the quality of the diffraction data, structures were phased using molecular replacement (MR) starting from either poly-alanine or poly-glycine models. A 1.2 Å electron density map generated from *in situ* diffraction data collected on a thaumatin crystal is shown in Figure 3B. From this process, the value of kinetic optimization and microfluidic methods in general can be appreciated: starting from purified protein solution, we were able to solve four structures in less than 5 days without ever directly handling a crystal.

Acknowledgment. This work was funded by National Institutes of Health (R01 HG003594, R01-CA77373), the Natural Sciences and Engineering Research Council of Canada (J. Payette Fellowship), the American Cancer Society (PF-03-124-01-GMC), the Mathers Foundation, and the National Cancer Institute (CA92584).

Supporting Information Available: Details of device fabrication, crystallization, scale-up experiments, cryoprotectant addition, harvesting procedures, cryogenic freezing, diffraction data statistics, and structure determination. This material is available free of charge via the Internet at <http://pubs.acs.org>.

References

- Hansen, C. L.; Skordalakes, E.; Berger, J. M.; Quake, S. R. *Proc. Natl. Acad. Sci. U.S.A.* **2002**, *99*, 16531–16536.
- Hansen, C.; Sommer, M. O.; Quake, S. R. *Proc. Natl. Acad. Sci. U.S.A.* **2004**, *101*, 14431–14436.
- Zheng, B.; Roach, L. S.; Ismagilov, R. F. *J. Am. Chem. Soc.* **2003**, *125*, 11170–11171.
- Zheng, B.; Tice, J.; Roach, L. S.; Ismagilov, R. F. *Angew. Chem., Int. Ed.* **2004**, *43*, 2508–2511.
- Xiao, T.; Takagi, J.; Wang, J.; Springer, T. *Nature* **2004**, 431.
- Perkel, J. M. *Scientist* **2004**, *18*, 44.
- Andrew, S. P. S. *Chem. Eng. Sci.* **1955**, *4*, 269–272.
- Merkel, T. C.; Bondar, V. I.; Nagai, K.; Freeman, B. D.; Pinnau, I. *J. Polym. Sci.* **2000**, *38*, 415–434.
- McPherson, A. *Crystallization of Biological Macromolecules*, 1st ed.; Cold Spring Harbor Laboratory Press: Cold Spring Harbor, New York, 1999.
- Luft, J. R.; DeTitta, G. T. *Methods Enzymol.* **1997**, *276*, 110–130.
- Yadav, M. K.; Gerds, C. J.; Sanishvili, R.; Smith, W. W.; Roach, L. S.; Ismagilov, R. F.; Kuhn, R.; Stevens, R. C. *In situ* data collection and structure refinement from microcapillary protein crystallization. *J. Appl. Crystallogr.* **2005**, *38*, 900–905.

JA0576637